

Effect of the particle shape on the particle dynamics in a spheronization process

Dominik Weis^{1,*}, Maria Niesing², Markus Thommes², and Sergiy Antonyuk¹

¹Institute of Particle Process Engineering, University of Kaiserslautern, 67663 Kaiserslautern, Germany

²Chair of Solids Process Engineering, Technical University Dortmund, 44227 Dortmund, Germany

Abstract. Spherical granules with a narrow size distribution are widely used in many pharmaceutical applications. Extrusion-spheronization is a well-established process to produce such pharmaceutical pellets. The cylindrical extrudates from the extrusion step are rounded in the spheronizer. The formation mechanisms inside of a spheronizer depend strongly on the particle dynamics. To describe the complex particle flow and interactions, the Discrete Element Method can be used. In our previous works the spherical particles during the last part of the spheronization process were studied. Since the pellets have a cylindrical shape at the beginning and undergo different stages of deformation during the rounding process, the objective of this study was the description of the influence of the particle shape on the particle dynamics. To predict the interactions of the pellets, their dominant plastic behaviour was described with an appropriate contact model and the material parameters were calibrated with compression and impact tests.

1 Introduction

Spherical granules with a narrow size distribution and a homogeneous surface are highly interesting for pharmaceutical applications. To produce such pharmaceutical pellets, a combined extrusion and spheronization process is widely used [1-3]. A spheronizer consists of a stationary cylindrical wall and a rotating disk with a structured surface called friction plate (Figure 1).

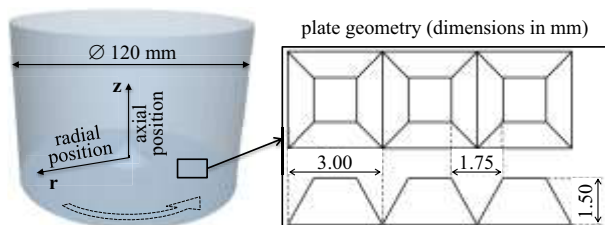


Fig. 1. Spheronizer geometry used in the simulations

The rounding of the wet cylindrical extrudates in the spheronization process is influenced by various interfering mechanisms. An important factor affecting those mechanisms is the particle dynamics in the spheronizer, which depends on the process conditions and the pellet properties. For this purpose, simulations of the particle dynamics were performed with the Discrete Element Method (DEM). In our previous work, the particle dynamics for different process conditions and material properties were studied for a late stage of the spheronization process, in which our particles can be approximated as spheres. [4]. Since the pellets have a cylindrical shape at the beginning of the spheronization process and undergo different stages of deformation

(cylindrical – dumbbell - spherical) during the rounding process [5-7], this contribution focuses on the influence of the particle shape on the particle dynamics. The simulation results provide information about the influence of the particle shape on the particle flow regime and the mixing of the particle torus, as well as the influence on the collision rates and forces. This information obtained on the micro scale can be used as the basis to describe the overall rounding process on the macro scale for example with a population balance model as it was done in [8] for a melt granulation process. To calibrate the contact model for the simulations, the dominant plastic behaviour of the pellets was investigated in experiments. The required material parameters were derived by compression and impact tests with spheronized pellets.

2 Materials and methods

2.1 Material properties of pharmaceutical pellets

The studied pellets were produced by extrusion/spheronization. A mixture consisting of microcrystalline cellulose (Vivapur 102, JRS Pharma, Germany) with a mass fraction $w_i = 0.2$ g/g and α -lactose monohydrate (Granulac 200, Meggle, Germany) with $w_i = 0.8$ g/g was extruded (Micro 27 GL-28D, Leistritz, Germany) with water at 300 rpm. Afterwards, 450 g of the extrudates were spheronized in a lab scale spheronizer (RM300, Schlüter, Germany) with a rotational speed of the friction plate of 750 rpm for 5 minutes. The deformation behaviour of spheronized pellets was obtained with

* Corresponding author: dominik.weis@mv.uni-kl.de

uniaxial compression tests. A single pellet was loaded by a punch with a rate of 20 $\mu\text{m/s}$ while the force and displacement were continuously recorded. Moreover, loading/unloading tests were performed. The pellet was loaded up to a predefined maximal force of 0.1 N. From measured force-displacement curves, the important parameters like stiffness and static coefficient of restitution were estimated. Figure 2 shows a typical force-displacement curve of the tested pellets. It exhibits the dominant plastic material behaviour.

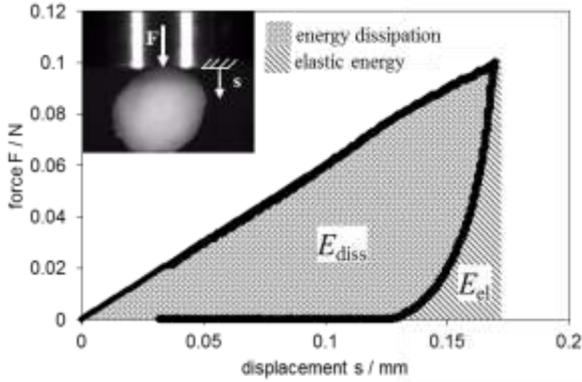


Fig. 2. Typical force-displacement curve obtained by uniaxial compression test

The energy dissipation based on plastic deformation can be expressed with a static restitution coefficient e_{stat} :

$$e_{\text{stat}} = \sqrt{\frac{E_{\text{el}}}{E_{\text{load}}}} = \sqrt{\frac{E_{\text{el}}}{E_{\text{diss}} + E_{\text{el}}}} \quad (1)$$

For dynamic impacts, the energy dissipation can be different, due to viscous effects [9]. For this reason, additional impact tests are necessary. Normal collisions with impact speeds of 0.3 - 0.6 m/s on the horizontal surface of the pyramids of the friction plate were recorded with a high speed camera (Y 8 Speedgrade 3, IDT, Tallahassee, US). The restitution coefficient was calculated as a ratio of the rebound and impact velocities. The results of the compression and impact tests are shown in Table 1. Due to the small deviation of the results obtained by compression and impact tests, viscous effects can be assumed to be negligible.

Table 1. Material parameters of pellets obtained by compression and impact experiments

parameter	unit	arithmetic mean	standard deviation
pellet diameter	mm	1.364	0.137
e_{stat} (compression)	-	0.227	0.035
e_{dyn} (impact)	-	0.218	0.056
breakage force	N	0.146	0.031
loading stiffness	N/mm	0.658	0.164

2.2 Discrete Element Method

The DEM, introduced firstly in 1979 by Cundall and Strack [10], can be used to simulate the dynamics of

particulate systems. The method describes each particle in the system and its interactions with other particles or rigid walls via contact forces F_c . The particles are assumed to be spherical and indestructible. Based on the force balance for every single particle, the equations of motion (2) and (3) are numerically solved.

$$m_p \frac{dv_p}{dt} = F_g + \sum_i^k F_{c,i} \quad (2)$$

$$J_p \frac{d\omega_p}{dt} = \sum_i^k M_{p,i} \quad (3)$$

In the equations m_p and J_p are the mass of a particle and its moment of inertia while v_p and ω_p are the velocity and the angular velocity. $F_{c,i}$ and $M_{p,i}$ are the force and the torque acting on a particle due to the interactions with contact partner i . These contact forces need to be modeled with an appropriate contact model. To describe the dominant plastic material behavior of the pellets used in this study, the model of Walton and Braun [11-13] can be utilized. It has a linear force-displacement relationship and can be assigned to the hysteresis models. That means the energy dissipation due to plastic deformation is modeled by assuming different stiffnesses K_1 and K_2 for loading and unloading. The force-displacement curve is shown in Figure 3. It can be seen that for a reloading, before an interaction is finished, the greater stiffness K_2 is used because of the local consolidation in the contact area. The normal force can therefore be calculated as follows:

$$F_{c,n} = \begin{cases} K_1 \cdot s_n & \text{if } K_1 \cdot s_n < K_2 \cdot (s_n - s_0) \\ K_2 \cdot (s_n - s_0) & \text{if } s_n > s_0 \\ 0 & \text{if } s_n \leq s_0 \end{cases} \quad (4)$$

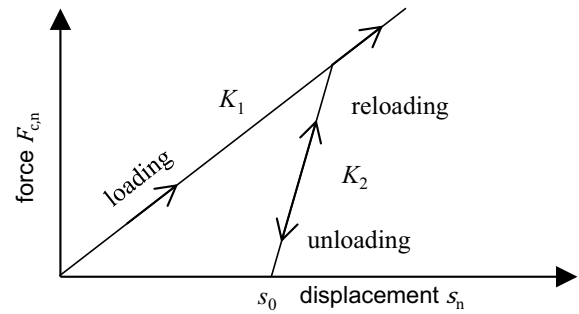


Fig. 3. Force-displacement curve of Walton and Braun model

Since the model does not include energy dissipation based on viscous damping terms, the relationship in (5) can be derived between the stiffness of the loading and unloading case. With a constant value for the coefficient of restitution the unloading stiffness can be calculated from the loading stiffness.

$$e = \sqrt{\frac{K_1}{K_2}} \quad (5)$$

In DEM there are different methods to approximate the real, non-spherical shape of particles. Generally there are two strategies to model the real particle shape: the single-particle and the clustered-particle approach [14]. In this study the clustered-particle approach, in which smaller spherical particles are connected in order to form a particle of complex shape [15, 13], is used because it is

a relatively simple model, which can approximately predict the dynamic of non-spherical particles [17].

3 Results

The three different stages of the pellet rounding, which can be seen in Figure 4 (left: cylindrical, mid: dumbbell, right: spherical), were simulated in this study. For every particle shape the pellets had a diameter of 1 mm. Simulations were performed with a bed mass of $m = 35$ g and a rotational speed of the plate of $n = 2500$ rpm. Since, during spheronization, the bed mass remains constant and breakage of cylindrical particles takes places, the total number of pellets in the simulation of dumbbell and spherical stages was assumed to be higher than for the cylindrical stage.

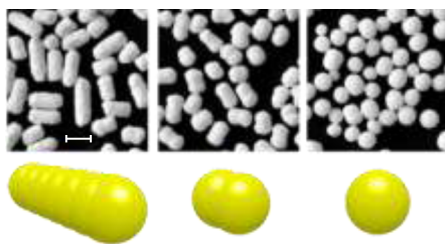


Fig. 4. Pellets after spheronization times of 20, 120, 480 s [18] modelled with the multi-sphere approach, (scale: 2.0 mm)

Figure 5 shows the residence probabilities of the different shaped pellets in a poloidal cut plane. As can be seen on the left side, a poloidal cut plane is a rz -cut through the particle torus. Due to the rotational symmetry, such a poloidal cut plane is representative for the whole particle bed. The residence probabilities, defined as the average number of particles in the different regions scaled with the total number, exhibit a decrease in the bed porosity with increasing sphericity of the particles. For every particle shape, there is a zone with very small values for the residence probability close to the friction plate. This zone shows the biggest axial expansion for the cylindrical particles and decreases with increasing sphericity. It is also noticeable that the spherical particles are regularly arranged close to the wall. Those maxima in the residence probability get less and less with decreasing sphericity. The influence of the particle shape on the rate of the collisions of particles with the friction plate is shown in Figure 6. The collision

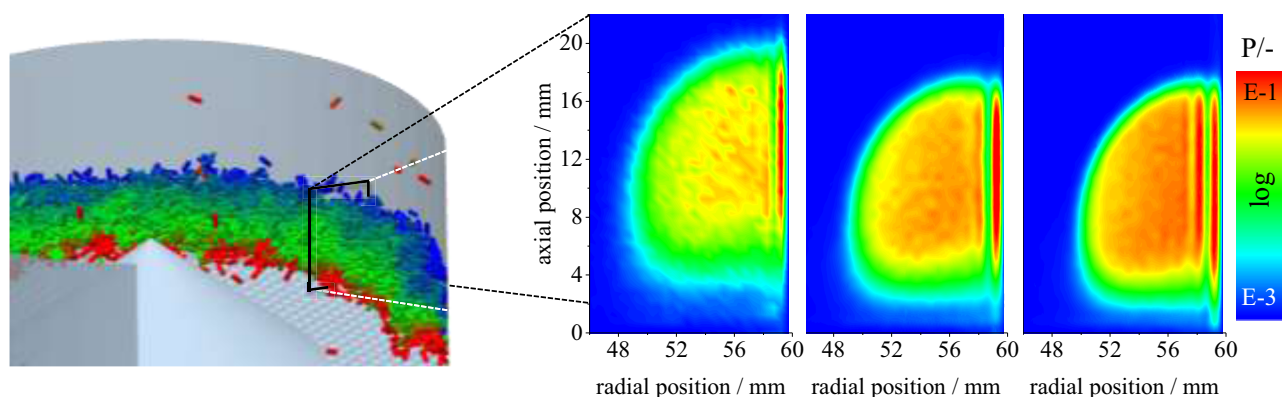


Fig. 5. Residence probability for different particle shapes (left: cylindrical, mid: dumbbell, right: spherical) in the poloidal cut plane

rate is defined as the number of collisions with the friction plate per particle within a second. All curves for the different particle shapes are qualitatively similar. The particles collide at the inner radial positions for the first time with the friction plate. The maximum of the collision rate is reached at about $r = 59$ mm for all studied particle shapes. In the middle of the torus, at $50 < z < 58$, no significant difference between the spherical and the dumbbell shape can be obtained. The cylindrical shaped particles collide more often with the friction plate in this region. In the region close to the wall, the dumbbell shaped particles collide less often with the friction plate compared to the other shapes.

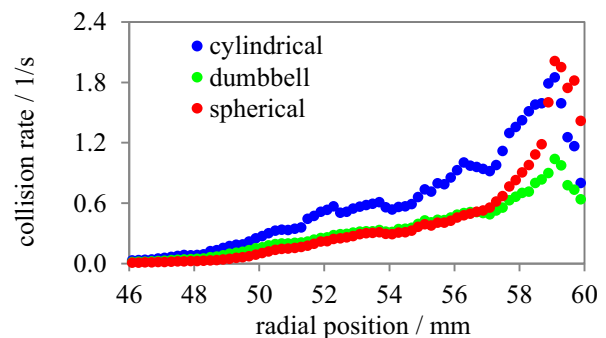


Fig. 6. Averaged rates of the collisions with the friction plate

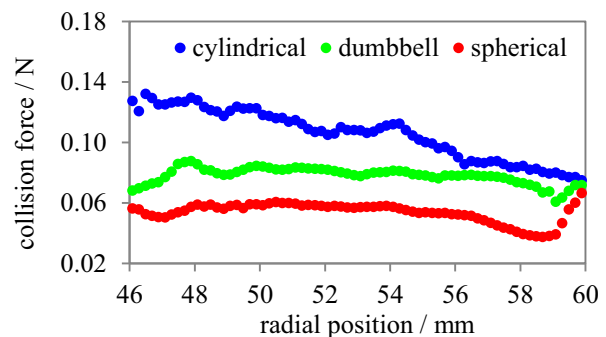


Fig. 7. Averaged forces of the collisions with the friction plate

Figure 7 shows the averaged collision force of the collisions of the different shaped particles with the friction plate. It can be seen that the biggest forces act on the cylindrical shaped particles. Both distributions, the collision rates and forces, are important functions to describe the overall rounding process in a spheronizer on the macro scale. For this reason the different rounding

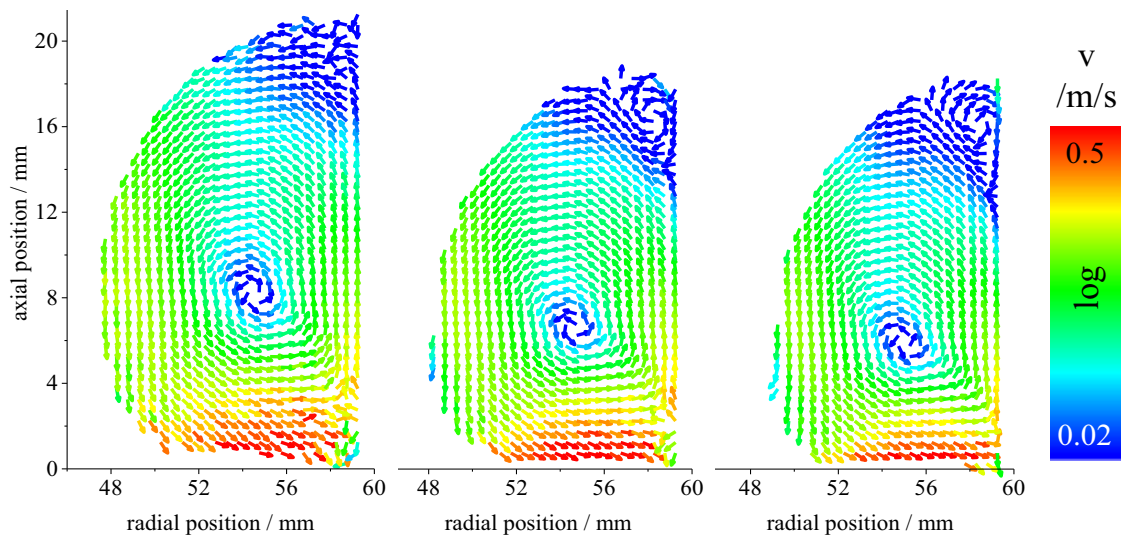


Fig. 8. Averaged poloidal particle movement for different particle shapes (left: cylindrical, mid: dumbbell, right: spherical) in the poloidal cut plane

mechanisms like deformation, attrition and breakage have to be described as a function of the collision forces and pellet shape and can then be used in a population balance. Comparing the breakage forces measured in the compression tests with spherical pellets in Table 1 for example, the simulation results indicate that no breakage will occur for the spherical shaped particles.

In Figure 8 the averaged poloidal velocity map is shown for the different shapes. The overall flow regime is quite similar. The largest poloidal velocities are reached in the region with high porosity close to the friction plate. In accordance to the axial expansion of this region for cylindrical particles, the region with high poloidal velocities also increases for cylindrical shaped particles. The primary rotational movement, which occurs for every particle shape, is superimposed by a smaller counter rotating movement at the top of the torus for the dumbbell and the spherical shape. For every particle shape, there are two zones which exhibit comparative small poloidal velocities, what has a negative effect on the mixing behaviour. The omission of the counter rotating movement at the top of the particle torus for the cylindrical particles should have positive effects on the mixing. Since we assume that the main part of the rounding happens due to the interaction with the plate, the mixing has also to be taken into account to describe the overall rounding process.

4 Conclusion

In this contribution the effect of the particle shape on the particle dynamics in a spheronization process is analysed with DEM simulations. For this reason the plastic material behaviour was described with an appropriate contact model. To calibrate the model, the required material parameters were determined by compression and impact tests with spheronized pellets. The different deformation stages were modelled using the multi-sphere approach. The simulations provide information about the residence probabilities and the flow regime of different shaped particles. Moreover the impact on the collision rates and forces of the collisions with the friction plate

were examined. The parameter obtained on the micro scale are the basis to describe the overall rounding in a spheronizer on the macro scale in a population balance model.

References

1. S. Muley, T. Nandgude, S. Poddar, Asian J. Biomed. Pharm. Sci. (to be published)
2. A. Bathool, G.D. Vishakante, M.S. Khan, V.K. Gupta, J. Pharm. Res. **4**, 3282-3286 (2011)
3. N. Shinde et al., Asian J. Res. Pharm. Sci. **4**, 38-47 (2014)
4. D. Weis, S. Antonyuk, D. Thaete, M. Thommes, Proceedings of IV International Conference on Particle-Based Methods, 576-578 (2015)
5. C. Krueger, M. Thommes, P. Kleinebudde, Powder Technol. **238**, 176-187 (2013)
6. C.L.S. Lau et al., Chem. Eng. Res. Des. **92**, 2413-2424 (2014)
7. M.P. Bryan et al., Powder Technol. **270**, 163-175 (2015)
8. H.S. Tan et al., Powder Technol. **143**, 65-83 (2004)
9. S. Antonyuk et al., Granular Matter **12**, 15-47 (2010)
10. P. A.Cundall, O. D. Strack, Geotechnique **29**, 47-65 (1979)
11. O. R. Walton, R. L. Braun, Acta Mechanica **63**, 73-86 (1986)
12. O. R. Walton, R. L. Braun, J. Rheol. **30**, 949-980 (1986)
13. O. R. Walton, Particulate two-phase flow **25**, 884-907 (1993)
14. D. Höhner et al., Powder Technol. **208**, 643-656 (2011)
15. J. Favier et al., Eng. Comput. **16**, 467-480 (1999)
16. M.H. Abbaspour-Fard, Biosystems Engineering **88**, 153-161 (2004)
17. D. Höhner et al., Powder Technol. **208**, 643-656 (2011)
18. M. Koester, E. Willemsen, C. Krueger, M. Thommes, Int. J. Pharm. **431**, 84-89 (2012)